Mechanism of circadian oscillation of the mammalian core clock gene *Per2*

（時計遺伝子 *Per2* の発現制御機構）

2014

跡部　祐太

Contents

Abstract

Daily rhythms in behavior and physiology are controlled by an internal self-sustained molecular oscillator, referred to as the circadian clock. Circadian rhythms are generated in a cell-autonomous manner through transcription/translation-based autoregulatory feedback loops, wherein protein products of three *Period* genes (*Per1*, *Per2* and *Per3*) periodically suppress their own transcription. Genetic studies have suggested that, of the three *Period* genes, *Per2* has a dominant role in both humans and mice. However, little is known about the regulatory mechanism underlying expression of this gene. In this thesis, I investigated the molecular mechanism driving the circadian transcription of the mouse *Per2* gene. I find that the *Per2* promoter contains a circadian *cis*-element, termed E'-box. Furthermore, I generated novel mutant mice carrying a point mutation in the E'-box sequence of the *Per2* promoter. Analysis of the mutant mice revealed a previously unknown *in vivo* function of this element in regulation of circadian transcription of the *Per2* gene.

Introduction

Daily rhythms in behavior and physiology are controlled by an internal self-sustained molecular oscillator, referred to as the circadian clock[1-5]. Circadian rhythms are generated in a cell-autonomous manner through transcription/translation-based autoregulatory feedback loops[5-8], wherein protein products of three *Period* genes (*Per1*, *Per2* and *Per3*) periodically suppress their own transcription (**Figure 1**). In this general model, the circadian positive regulators, CLOCK and BMAL1, promote transcription of the *Period* (*Per1*, *Per2*, and *Per3*) and *Cryptochrome* (*Cry1* and *Cry2*) genes through E-box *cis*-elements (5′-CACGT[G/T]-3′) located in their promoter regions. Once the repressor proteins, PER and CRY, reach a critical concentration, they form a complex and inhibit CLOCK:BMAL1-mediated transcription.

Genetic studies have suggested that, of the three *Period* genes, *Per2* has a dominant role in both humans and mice[9-12]. However, little is known about the regulatory machinery of *Per2*, although there are many studies describing *Per1* expression mechanism[13-16]. In this thesis, I investigated the molecular mechanism driving the circadian transcription of the mouse *Per2*

gene. I found that *Per2* promoter contains a circadian *cis*-element, termed E'-box (**Chapter 1**). Furthermore, I generated novel mutant mice carrying a point mutation in the E'-box sequence of the *Per2* promoter (**Chapter 2**). Analysis of the mutant mice revealed a previously unknown *in vivo* function of this element in regulation of circadian transcription of the *Per2* gene (**Chapter 3**).

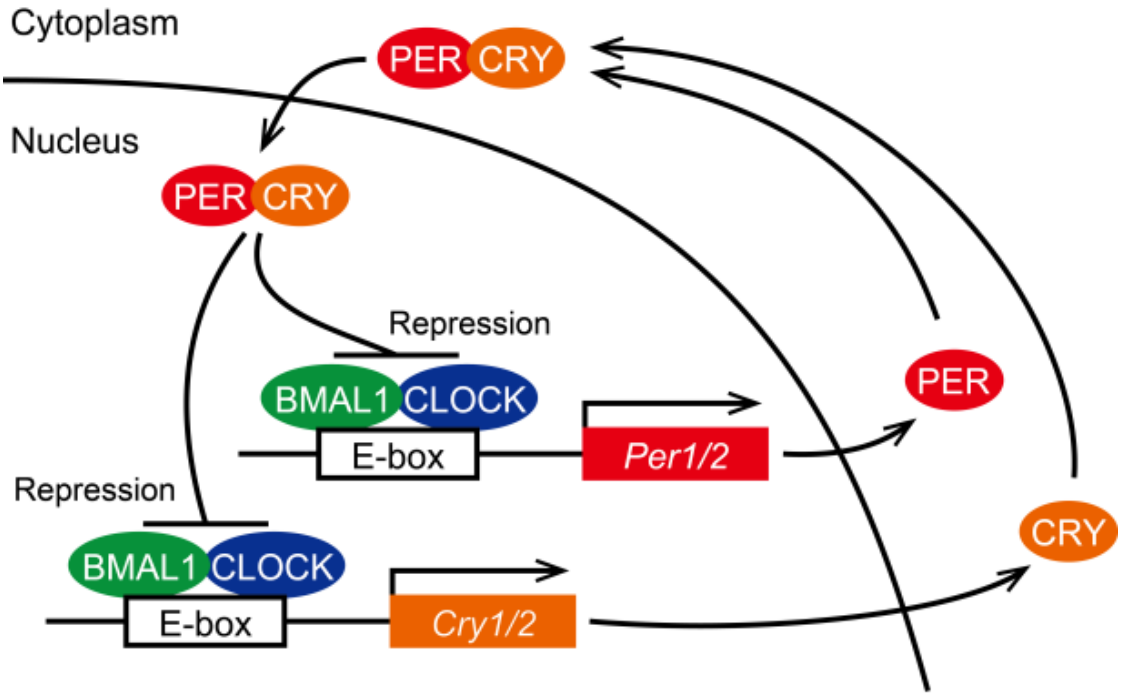

Figure 1. Autoregulatory feedback model of the mammalian cellular clock. The circadian clock mechanism involves transcription-translation feedback loops comprised of a set of core clock genes (see main text for details).

Materials and Methods

Antibody. PER2 antibodies were raised in rabbit using a GST-fused mPER2 protein fragment (a.a. 882-1258). The raised antibodies were affinity-purified using an MBP-fused mPER2 fragment (a.a. 882-1258).

Animals. Male mice at 7-8 weeks of age were housed in light-tight boxes and entrained to LD12:12 conditions. After a minimum of 7 days, animals were transferred to constant darkness (DD) conditions. Twelve hours after DD, tissues were collected every four hours over circadian cycles at CT0, CT4, CT8, CT12, CT16, and CT20 (CT represents circadian time; CT0 denotes the beginning of the subjective day and CT12 the beginning of the subjective night). All the studies were approved by the Animal Experimentation Committee of Kyoto University.

Western blot analysis. Western blotting was performed as described[17] with modifications. Livers from mice were immediately minced and homogenized in 1 ml per 50 mg liver block of 2× Laemmli sample buffer containing 2× cOmplete Protease Inhibitor

cocktail (Roche diagnostics) and 2× PhosSTOP Phosphatase Inhibitor cocktail (Roche diagnostics). After centrifugation at 12,000× *g* for 10 min, supernatant proteins were separated by electrophoresis through sodium dodecyl sulfate (SDS)–6% polyacrylamide (120:1, acrylamide:bis-acrylamide) gels and then transferred into PVDF membranes. Imunoreactivities to anti-PER2 antibody were visualized with enhanced chemiluminescence using horseradish peroxidase-conjugatged anti-rabbit IgG antibody (GE healthcare).

Laser microdissection of the SCN. Mice were sacrificed by cervical dislocation, and the brains were frozen immediately on dry ice. A series of cryosections (30 μm thick) containing the mouse SCN were mounted onto FrameSlides (POL-membrane 0.9 mm; Leica) and fixed with EtOH: Acetate (19:1) for 3 min at 4°C. After washing with cold RNase free water, sections were stained with 0.05% toluidine blue and quickly air-dried. The SCN was isolated from 10 to 15 serial sections per brain using a LMD device (Leica; 10× magnification) and lysed into a Trizol reagent. All procedures were finished within 20 min per brain. Typical yield of purified

total RNA was about 50 ng per SCN.

RNA extraction and quantitative reverse transcription-PCR (qRT-PCR). RNA was extracted using an RNeasy kit (Qiagen) according to the manufacturer's instruction. Total RNA was converted to cDNA with SuperScript VILO cDNA Synthesis kit (Invitrogen), and quantitative PCR (qPCR) was run in duplicate with a Platinum SYBR green qPCR SuperMix-UDG kit (Invitrogen) and a set of primers shown below. As a qPCR device, I used a StepOnePlus real-time PCR monitoring system (Applied Biosystems), and quantification of target cDNAs was achieved with a standard curve method as described previously[18]. The data were normalized to those of *Rplp0*. The sequences for the primers are as follows: for *Per2*, forward primer 5'-GGA AAC GAG AAC TGC TCC AC-3' and reverse primer 5'-GCT CTG CCT CTG TCA TCA TG-3'; for *Per2*-intron, forward primer 5'-CAG ATG GAC TGG GAG TAT GTC A-3' and reverse primer 5'-AGC CAA GGT ATG TCT CAA AGG A-3'; for *Per3*, forward primer 5'-CCC TAC GGT TGC TAT CTT C-3' and reverse primer 5'-CTG GCA ACT TCT TTC GTT TGT TG-3'; for *Npas2*, forward primer 5'-GGA

CCA GTT CAA TGT TCT CAT C-3’ and reverse primer 5’-ACG ACG ATG ACG AAG CCA TC-3’;for *Dbp*, forward primer 5’-AAT GAC CTT TGA ACC TGA TCC CGC T-3’ and reverse primer 5’-GCT CCA GTA CTT CTC ATC CTT CTG T-3’; for *Rplp0*, forward primer 5’-CTC ACT GAG ATT CGG GAT ATG-3’ and reverse primer 5’-CTC CCA CCT TGT CTC CAG TC-3’.

qRT-PCR Screen with Fluidigm Dynamic Arrays. TaqMan qPCR analysis was performed on a BioMark HD System (Fluidigm), using a 48.48 Fluidigm BioMark Dynamic Array chip (Fluidigm) according to the manufacturer’s instructions. cDNA was pre-amplified for 14 cycles with a set of primers specific to the target genes (see below). Pre-amplified mixtures (total 36 samples: 6 time points × 2 genotypes × triplicate) were combined with a set of TaqMan probes and primers (total 32 sets: 16 genes × duplicate) on a 48.48 chip using an IFC-MX-I Controller (Fluidigm). PCR was run on a BioMark real-time PCR reader (Fluidigm). Ct values were obtained with the Fluidigm Real-Time PCR Analysis software (Fluidigm). ΔCt was calculated by subtracting the Ct values of *Rplp0* from the Ct values of the gene of interest. ΔΔCt was then

calculated by subtracting the mean of the lowest ΔCt values of WT mice (i.e., circadian peak values of WT) from the mean of ΔCt values of each sample. Fold change of the gene was calculated by the equation: $2^{-\Delta\Delta Ct}$. TaqMan probe and primer sets used were as follows; for *Rplp0*, probe, 6-FAM-TGG CAA TCC CTG ACG CAC CGC C-TAMRA, forward primer (fw): 5'-GCG TCC TCG TTG GAG TGA C-3', reverse primer (rv): 5'-AAG TAG TTG GAC TTC CAG GTC G-3'; for *Per1*, probe, 6-FAM-AGC CCC TGG CTG CCA TGG-TAMRA, fw: 5'-CAG GCT TCG TGG ACT TGA GC-3', rv: 5'-AGT GGT GTC GGC GAC CAG-3'; for *Per2*, probe, 6-FAM-AGG CAC CTC CAA CAT GCA ACG AGC C-TAMRA, fw: 5'-GCA CAT CTG GCA CAT CTC GG-3', rv: 5'-TGG CAT CAC TGT TCT GAG TGT C-3'; for *Per3*, probe, 6-FAM-TTC TGC TCA TCA CCA CCC TGC GGT TCC-TAMRA, fw: 5'-ACA GCT CTA CAT CGA GTC CAT G-3', rv: 5'-CAG TGT CTG AGA GGA AGA AAA GTC-3'; for *Cry1*, probe, 6-FAM-TGA TCC ACA GGT CAC CAC GAG TCA GGA A-TAMRA, fw: 5'-TAG CCA GAC ACG CGG TTG-3', rv: 5'-AGC AGT AAC TCT TCA AAG ACC TTC A-3'; for *Cry2*, probe, 6-FAM-AGG TCT CTC ATA GTT GGC AAC CCA

GGC-TAMRA, fw: 5’-TGG ACA AGC ACT TGG AAC GG-3’, rv: 5’-GGC CAG TAA GGA ATT GGC ATT C-3’; for *Clock*, probe, 6-FAM-ACC CAG AAT CTT GGC TTT TGT CAG CAG C-TAMRA, fw: 5’-TGG CAT TGA AGA GTC TCT TCC TG-3’, rv: 5’-GAG ACT CAC TGT GTT GAT ACG ATT G-3’; for *Npas2*, probe, 6-FAM-TGG CTC TGT GCA TAC TTG ACT TGC CGT C-TAMRA, fw: 5’-CCA GCC CAT CCA GCC TAT GA-3’, rv: 5’-GCT GTT GGT AGG GTG TGA GTC-3’; for *Arntl1*, probe, 6-FAM-CGC CAA AAT AGC TGT CGC CCT CTG ATC T-TAMRA, fw: 5’-GTA CGT TTC TCG ACA CGC AAT AG-3’, rv: 5’-GTA CCT AGA AGT TCC TGT GGT AGA-3’; for *Arntl2*, probe, 6-FAM-ACC ACT TCC CGG TGA CAG TGC CCA-TAMRA, fw: 5’-AGC ACT GAA CCC GCC CAC-3’, rv: 5’-GCA GCC ATG TCT ATG CTG TCA-3’; for *Dbp*, probe, 6-FAM-CGG CTC CCA GAG TGG CCC GC-TAMRA, fw: 5’-CGG CTC TTG CAG CTC CTC-3’, rv: 5’-GTG TCC CTA GAT GTC AAG CCT G-3’; for *Nfil3*, probe, 6-FAM-CAG GGA GCA GAA CCA CGA TAA CCC ATG A-TAMRA, fw: 5’-CGC CAG CCC GGT TAC AG-3’, rv: 5’-CAT CCA TCA ATG GGT CCT TCT G-3’; for *Rorα*, probe, 6-FAM-TGG CAG AAC TAG

AAC ACC TTG CCC AGA A-TAMRA, fw: 5'-GAG AGA CTT CCC CAA CCG TG-3', rv: 5'-CTG GCA GGT TTC CAG GTG G-3'; for *Nr1d1*, probe, 6-FAM-CCC TGG ACT CCA ATA ACA ACA CAG GTG G-TAMRA, fw: 5'-TCA GCT GGT GAA GAC ATG ACG-3', rv: 5'-GAG GAG CCA CTA GAG CCA ATG-3'; for *Bhlhe40*, probe, 6-FAM-CCT CAC GGG CAC AAG TCT GGA AAC CTG-TAMRA, fw: 5'-AGC GGT TTA CAA GCT GGT GAT-3', rv: 5'-GGT CCC GAG TGT TCT CAT GC-3'; for *Bhlhe41*, probe, 6-FAM-TCT TCT GAT GCT GCT GCT CAG TTA AGG C-TAMRA, fw: 5'-ACA TCT GAA ATT GAC AAC ACT GGG-3', rv: 5'-GCG CTC CCC ATT CTG TAA AG-3'.

Plasmid construction. A 1.7-kb fragment upstream of mouse *Per2* transcription start site was PCR amplified from a bacterial artificial chromosome (BAC) clone (RP23-343F13, BACPAC). A point mutation of E'-box (–20 to –15, +1 corresponds to the transcription start site) was introduced using overlap extension PCR with synthetic oligonucleotide primers containing a mutant E'-box sequence. Then, the 1.7-kb fragment was obtained by digestion with *Bgl*II and cloned into pGL4.10.

Cell culture, transfection and realtime monitoring of luciferase activity in living cells. Mouse embryonic fibroblasts (MEFs) were cultured in Dulbecco's modified Eagle medium (D-MEM)–F-12 medium (Invitrogen) supplemented with 10% fetal bovine serum (FBS) and 1% penicillin-streptomycin-amphotericin. MEFs were transfected with *Per2*-1.7kb-Luc or *Per2*-mut1.7kb-Luc using Lipofectamine 2000 reagent (Invitrogen) according to the manufacturer's instruction, and incubated in phenol-red free D-MEM–F-12 supplemented with 10% FBS and 1% PSA premix for three days. The cells were then synchronized by a medium change, with 200 nM dexamethasone (Sigma-Aldrich) for 2 hr. Medium was then replaced with new medium containing 1 mM luciferin and luminescence was recorded in a luminometer-incubator at 37°C (Kronos DIO, ATTO) in successive bins of 20 min.

Generation of *Per2* E'-box (–20/–15) mutant mice. The targeting vector to generate *PB* mutant allele of *Per2* was constructed by using a Red/ET recombination system (Gene Bridges). The bacterial artificial chromosome (BAC) containing *Per2* was

obtained from BACPAC Resources at the Children's Hospital and Research Center at Oakland (RP23-343F13). Using a Red/ET method (Gene Bridges), a 10 kb genomic region of *Per2* (–5,899 to +4,103; +1, the transcription start site) that corresponds to the region of 6.5 kb upstream (long arm) and 3.5 kb downstream (short arm) of the *Per2* E'-box (–20/–15) was cloned into a vector containing a diphtheria toxin A gene (pDTA vector). Then, a modified *Per2* fragment (−90 to +650) that bears a mutated E'-box (GCTAGT) at −20/−15 with a *piggyBac* neomycin cassette at the TTAA quadruplet sequences (+600/+650) was created by multi-step fusion PCR. Here, the neomycin cassette is flanked by the *PB* terminal repeat sequences obtained from pIR-Vitro1-neo-mcs vector[19]. By a second-round Red/ET recombination, this fragment was recombined into the pDTA-10 kb *Per2* BAC vector. Full DNA sequences of the resultant *Per2* targeting vector were verified by DNA sequencing.

Gene targeting was carried out in TT2 cells, an embryonic stem cell line established from F1 embryo between C57BL/6J female and CBA male[20]. Chimeric males were bred to wild type C57BL/6J females producing F1N0 progeny. Germline

transmission was verified by PCR as well as Southern blot analysis of tail DNA. F1 heterozygous males were intercrossed with ROSA26-PBase knock-in mice[21] (a gift from A. Bradley, Wellcome Trust Sanger Institute, Hinxton, UK) to remove the *PB*-flanked neomycin cassette from the genome. A seamless excision of the neomycin cassette was confirmed by Southern blotting, PCR, and direct DNA sequencing. Genotypes were also determined by allele-specific TaqMan qPCR using the following probes: for wild-type (WT), 5'-FAM-TAG TGG AAA ACG TGA CCG C-MGB-3'; for mutant (Mut), 5'-VIC-TAG TGG AAA CTA GCA CCG C-MGB-3'. The use of different reporter dyes for each probe with separated emission wavelength maxima (probes for WT and Mut are labeled with FAM and VIC, respectively) enabled simultaneous monitoring of WT- and Mut-specific amplification in a single PCR with a common primer set used (forward: 5'-GGA GCC GCT AGT CCC AGT AG-3', and reverse: 5'-AGG TGG CAC TCC GAC CAA T-3'). The established mutant mice were backcrossed into the C57BL/6J background using a marker-assisted breeding (i.e., "speed congenic") approach[22, 23] as described[24] (Central Institute for Experimental Animals).

ChIP assay. Dual crosslinking ChIP assay was performed as described[25] with modifications. Briefly, livers from mice were immediately homogenized in 4 ml per liver of 1× PBS containing 2 mM disuccinimidyl glutarate (DSG), and the homogenates were kept at room temperature for 20 min. Formaldehyde was then added at a final concentration of 1% and incubated for a further 5 min. Crosslinking reactions were stopped by adding glycine (a final concentration, 150 mM) on ice. The homogenates (~5 ml per liver) were mixed with ice-cold 2.3 M sucrose buffer (10 ml per liver) containing 150 mM glycine, 10 mM HEPES [pH 7.6], 15 mM KCl, 2 mM EDTA, 0.15 mM spermine, 0.5 mM spermidine, 0.5 mM DTT, and 0.5 mM PMSF and layered on top of a 5 ml cushion of 1.85 M sucrose buffer (containing the same ingredients and including 10% glycerol), then centrifuged at 105,000× *g* for 1 h at 4°C in a Beckman SW28 rotor. The resultant nuclear pellets were washed twice with TBSE buffer (10 mM Tris-HCl [pH 7.5], 150 mM NaCl, 2 mM EDTA), transferred to a 1.5 ml siliconized tube, and stored at −80°C until use. The nuclei were resuspended in 1.5 ml per liver of IP buffer (10 mM Tris-HCl [pH 7.5], 150 mM NaCl, 1 mM EDTA, 1% Triton X-100, 0.1% sodium deoxycholate,

1 mM PMSF, and a protease inhibitor cocktail) and sonicated 80 times for 15 s each time at 4ºC using a Bioruptor UCW-201TM apparatus (Tosho Denki, Yokohama, Japan). For each assay, approximately 10 μg of fragmented chromatin (resuspended in 500 μl of IP buffer) was pre-cleared by incubating with 40 μl of protein A-agarose (Roche) for 2 h at 4°C on a rotating wheel. Pre-cleared chromatin was then incubated with the following antibody: for PER1, 2 μl of anti-mPER1 rabbit antiserum (#AB2201; MILLIPORE); for CRY1, 1 μg of affinity-purified anti-mCRY1 guinea pig polyclonal antibody (a kind gift from Dr. Choogon Lee); and for CRY2, 1 μg of affinity-purified anti-mCRY2 guinea pig polyclonal antibody (a kind gift from Dr. Choogon Lee), at 4°C overnight on a rotating wheel. Then, 40 μl of Protein A/G Plus-agarose (Santa Cruz) was added to each sample and the mixture was incubated for 1.5 h at 4°C. Beads were washed twice with IP buffer, twice with high salt buffer (20 mM Tris-HCl [pH 7.5], 500 mM NaCl, 2 mM EDTA, 1% Triton X-100, 1 mM PMSF), twice with LiCl buffer (20 mM Tris-HCl [pH 7.5], 250 mM LiCl, 2 mM EDTA, 0.5% Igepal CA-630, 1% sodium deoxycholate, 1 mM PMSF), and once with TE (10 mM Tris-HCl

[pH 7.5], 1 mM EDTA). Co-immunoprecipitated DNA fragments were eluted with 100 μl of 20 mM Tris-HCl [pH 7.5], 5 mM EDTA, 0.5% SDS, then reverse crosslinked at 65ºC for overnight, incubated with 10 μg of RNaseA for 30 min at 37ºC, with 50 μg of proteinase K for 90 min at 55ºC, and then purified using a Qiaquick Nucleotide Removal Kit (Qiagen). Immunoprecipitated DNA fragments were quantified by qPCR using THUNDERBIRD SYBR qPCR Mix (TOYOBO) with the following primer set: for *Per2* E'-box, forward primer 5′-GAG GTG GCA CTC CGA CCA ATG-3′ and reverse primer 5′-GCG TCG CCC TCC GCT GTC AC-3′; for *Per2* −4.5kb (negative binding site), forward primer 5′-CCA CAC GGT ACT CAG CGG GC-3′ and reverse primer 5′-GGG TCA CTG CGA GCC TTG CC-3′; for *Dbp* E-box, forward primer 5′-CCA CAC GGT ACT CAG CGG GC-3′ and reverse primer 5′-GGG TCA CTG CGA GCC TTG CC-3′; for *Dbp* +4.4kb (negative binding site), forward primer 5′-CCA CAC GGT ACT CAG CGG GC-3′ and reverse primer 5′-GGG TCA CTG CGA GCC TTG CC-3′.

Results

Chapter 1: Autoregulatory feedback model of *Per2* transcription through E'-box

Firstly, I sought to determine the circadian oscillation profiles of *Per2* mRNA and protein in the mouse liver. Mice were sacrificed at 4 h intervals over a 24-h cycle. Quantitative RT-PCR and Western blot analyses revealed that the levels of *Per2* mRNA and protein exhibit an overt circadian oscillation with a typical phase-relationship (**Figure 2**). The PER2 protein began to increase 4 hours behind mRNA expression and reached its peak when the mRNA levels were decreasing. These observations corroborate the current negative feedback model, in which PER2 represses its own transcription. In an attempt to further test this model, I next explored the regulatory *cis*-element on the *Per2* promoter. Mouse embryonic fibroblasts were transfected with a luciferase reporter vector containing a 1.7-kb fragment of the 5'-flanking region of *Per2* (**Figure 3a**), and its promoter activity was monitored using a realtime luminometer system. I observed a robust circadian oscillation of the *Per2* promoter activity over four cycles (**Figure**

3b). Furthermore, I demonstrated that a single point mutation that was introduced into the E'-box sequence located in the vicinity of the transcription start site of *Per2*[26, 27] resulted in a complete abrogation of this rhythmicity (**Figure 3b**). These *in vitro* data strongly suggest that this single E'-box element is indispensable for the circadian activation and repression of *Per2* gene.

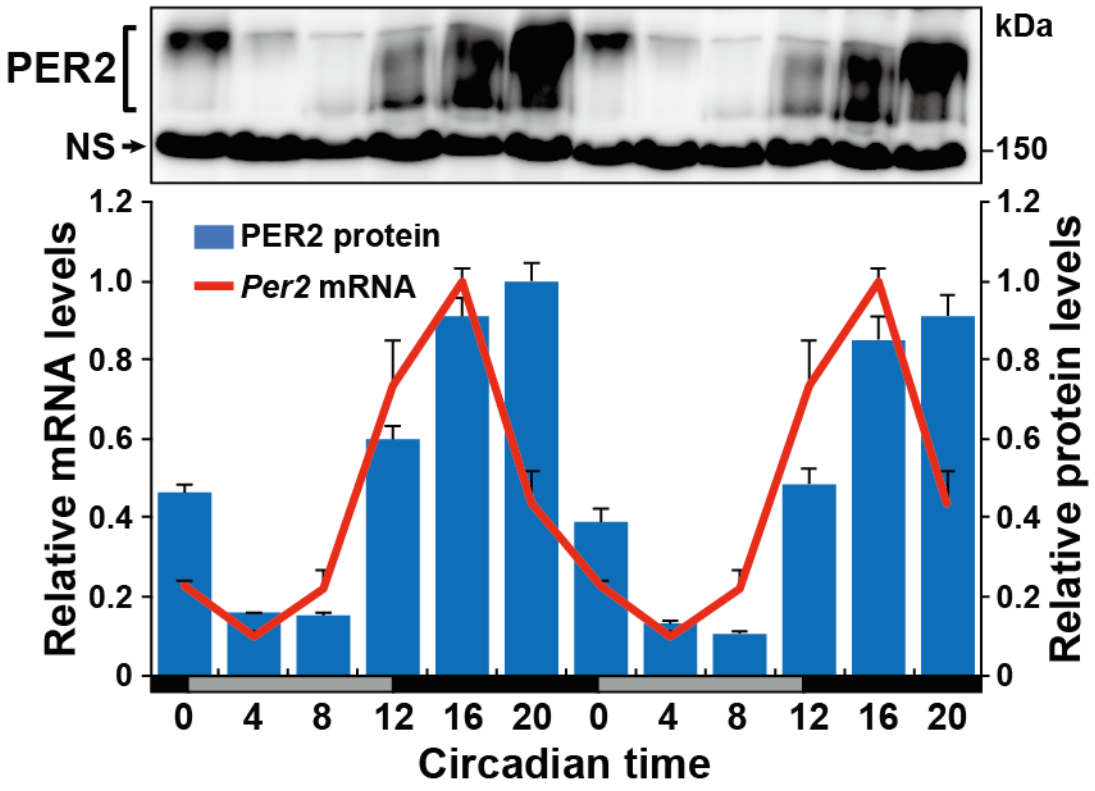

Figure 2. Circadian expression profiles of *Per2* mRNA and protein in mouse liver. Mice were sacrificed every four hours over two circadian cycles in DD, and whole liver lysates were subjected to immunoblotting with anti-PER2 antibody. The bar graph shows relative band intensities. Values were determined by densitometry and expressed as the means ± variation from two independent experiments. NS, nonspecific band as loading control. The red line shows a double-plotted circadian expression profile of the *Per2* mRNA in the liver. Relative *Per2* mRNA levels were determined by qRT-PCR. Values are means ± variation (n = 2 mice for each data point) normalized to expression of ribosomal protein large P0 (Rplp0)-encoding gene.

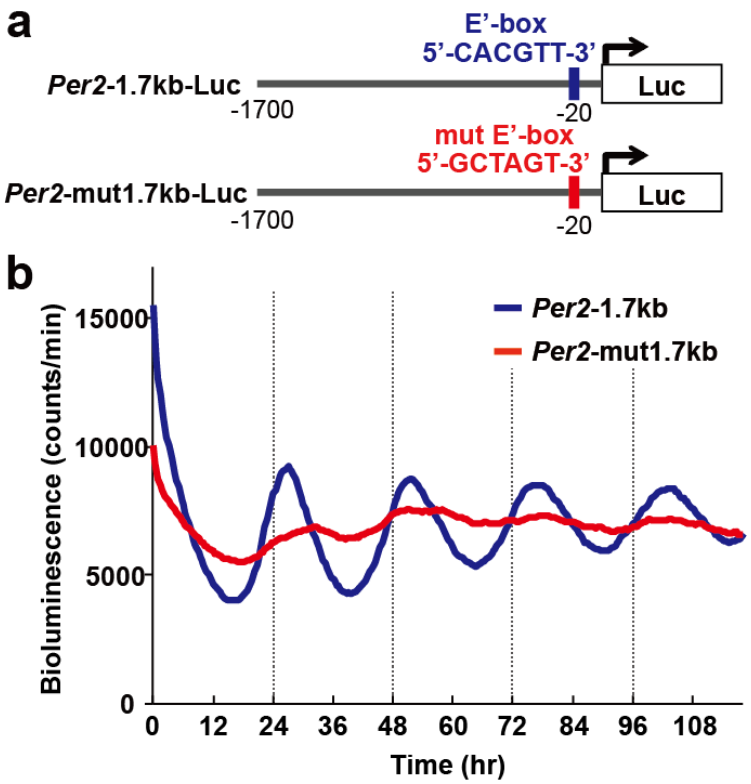

Figure 3. The E'-box is required for the circadian cycle of the *Per2* promoter-driven reporter gene expression. a, Schematic representation of luciferase reporter constructs containing 1.7-kb mouse *Per2* gene promoter with or without introduction of a mutation at the E'-box. **b,** Bioluminescence records of mouse embryonic fibroblasts transiently transfected with either wild-type (*Per2*-1.7kb) or mutant (*Per2*-mut1.7kb) reporter vector. Cells were synchronized with dexamethasone treatment for 2 h. Then, medium was replaced with luciferin-containing medium, and luminescence was recorded in successive bins of 20 min.

Chapter 2: Generation of mice carrying a point mutation of the *Per2* E'-box

To investigate the role of E'-box in regulation of *Per2* oscillation *in vivo*, I generated *Per2* E'-box mutant mice. To introduce a point mutation into this element, I employed a *piggyBac* (*PB*) transposon system. *PB* is a moth-derived DNA transposon[28] whose functionality is retained in mammals[29, 30]. Unlike the well-established methods relying on the Cre/*loxP* and Flp/*FRT*-based recombination systems[31, 32], PB transposase (PBase)/*PB*-based system achieves a 'seamless' excision of a *PB*-flanked target sequence without any residual 'footprint'[28, 30]. This allows, for example, 'complete' removal of a neomycin resistant gene-coding cassette from a mutant mouse genome without leaving any unwanted residual sequence[33, 34]. I therefore constructed a targeting vector, carrying a mutant E'-box sequence and a neomycin resistant cassette flanked by *PB* terminal repeats (**Figure 4a**). Targeted mouse embryonic stem cell clones were injected into blastocysts to generate chimeric mice. To remove the *PB*-flanked neomycin cassette from the genome, F1 heterozygotes were intercrossed with

ROSA26-PBase mice that carry a ubiquitously expressed PBase gene at the ROSA26 locus[21]. I performed Southern blot analysis and confirmed that the neomycin cassette was deleted without reintegration into the host genome (**Figure 4b**). Finally, a seamless excision of the cassette was confirmed by DNA sequencing (**Figure 4c**). The sequence analysis also verified that a point mutation was indeed introduced into the E'-box (**Figure 4c**). Genotypes were also determined by allele-specific TaqMan qPCR (**Figure 4d**). Moreover, the established mutant mice were backcrossed to the C57BL/6J background, and at the end of backcrossing, I confirmed that 64 microsatellite markers covering all individual mouse chromosomes were replaced with those of the C57BL/6J mouse strain (**Figure 5**). Finally, homozygous mutation was confirmed by DNA sequencing (**Figure 4e**).

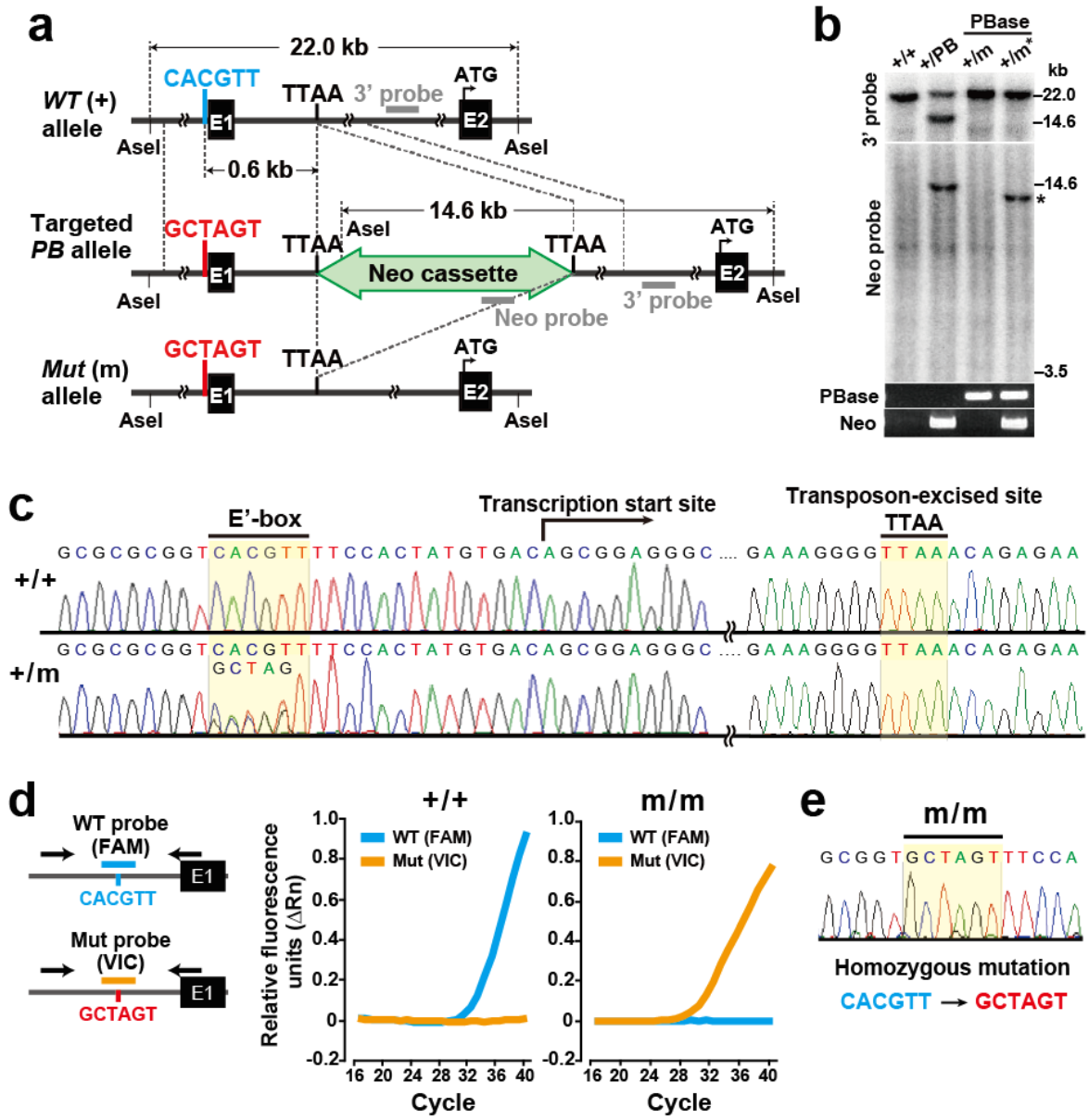

Figure 4. Generation of mice carrying a single mutation at the *Per2* E'-box (–20/–15). a, The strategy for precise genome modification using the *piggyBac* transposon. Top line, structure of the mouse *Per2* gene; E1, exon1; E2, exon2; Blue, wildtype E'-box (CACGTT). Red, mutant E'-box (GCTAGT). Green, *piggyBac* transposon carrying a neomycin resistant gene (Neo cassette), inserted at the TTAA site (+600/+650). Gray bars, Southern blot probes. **b**, Southern blotting and PCR analysis showing insertion (+/PB) and excision (+/m and +/m*) of the *piggyBac* transposon. *, a reintegrated Neo fragment. ***(legend continued on next page)***

c, Sequence analyses revealed precise modification of the E'-box and seamless excision of the *piggyBac* transposon from the TTAA site. Heterozygous mutant (+/m) sequences exhibit dual signals at the E'-box (CACGTT and GCTAGT). **d**, Genotyping of wildtype (+/+) and homozygous mutant (m/m) mice by allele-specific TaqMan qPCR. Amplification curves for wildtype (CAACGTT) and mutant (GCTAGT) sequences were measured using FAM-labeled WT probe (blue) and VIC-labeled mut probe (orange), respectively. Arrows, PCR primers. **e**, Sequence analysis of m/m mice. Homozygous mutation of the E'-box was confirmed.

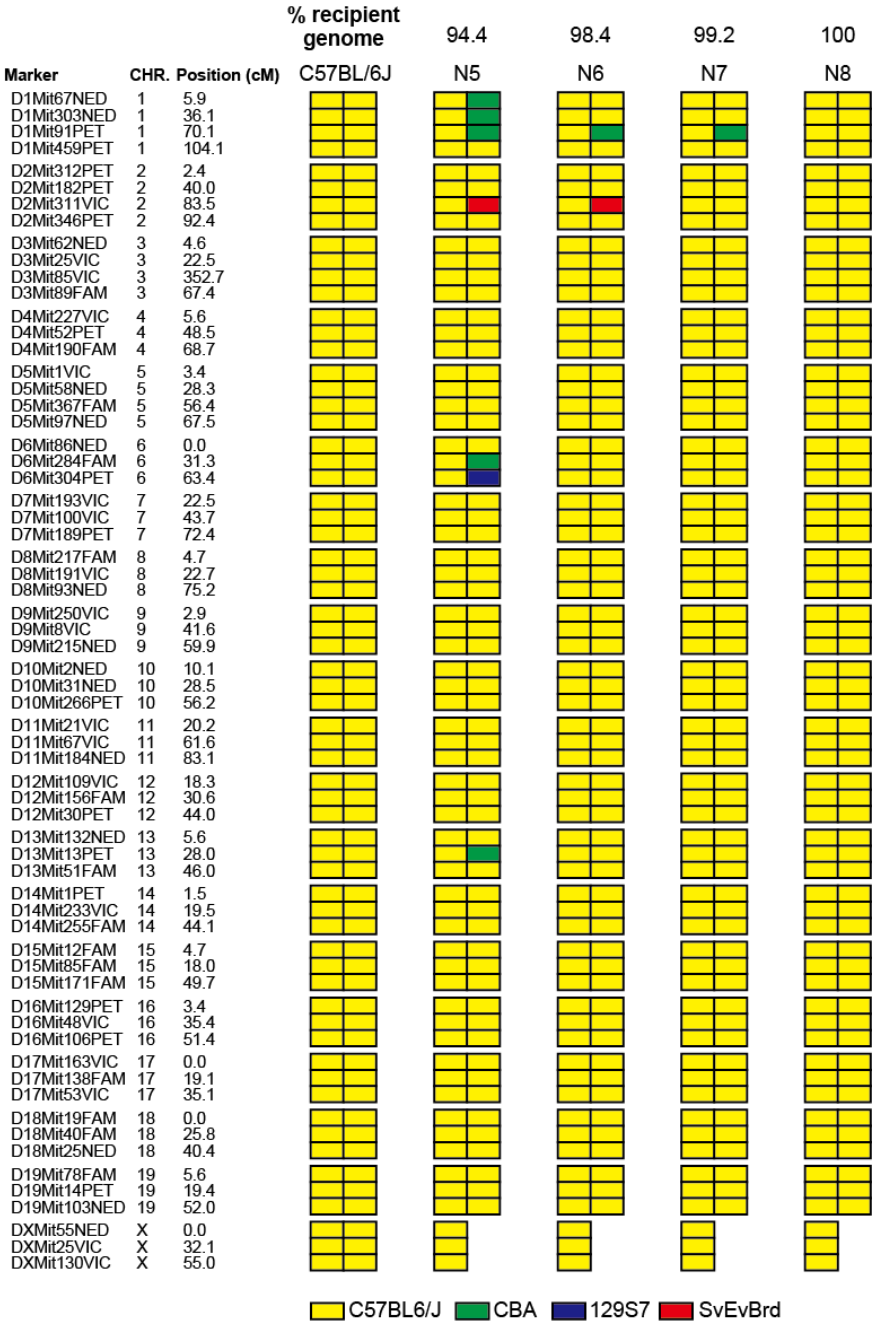

Figure 5. Marker-assisted backcrossing of *Per2* E'-box (−20/−15) mutant mice to C57BL/6J background. Genotypes of 64 microsatellite markers are color-coded: yellow, C57BL/6J; green, CBA (derived from TT2 ES cell); blue, 129S7 (derived from ROSA26-PBase mice); and red, SvEvBrd (derived from ROSA26-PBase mice). Backcross generations (N5 to N8) and deduced percentages of recipient genome are indicated at the top of each column.

Chapter 3: Characterization of *in vivo* role of the *Per2* E'-box

To evaluate whether the E'-box mutation *in vivo* abrogates rhythmicity of *Per2* expression, I measured circadian profiles of *Per2* mRNA in the mouse liver samples collected every 4 hours in constant darkness. Quantitative RT-PCR analysis revealed that the point mutation of the *Per2* E'-box caused alteration of the circadian rhythm of *Per2* (**Figure 6c**). This mutation impairs circadian repression of *Per2* expression and thereby elevates the levels of the baseline (**Figure 6d**). Similar results were obtained for the suprachiasmatic nucleus (SCN) in the brain (**Figure 6a, b**), which serves as the mammalian circadian center. Thus, the E'-box appears to be important for repression of *Per2* transcription *in vivo*.

To test the consequence of the altered *Per2* mRNA expression, I performed Western blot analysis to measure circadian profiles of the PER2 protein in the liver. Consistent with the impaired repression of *Per2* transcription in mutant mice, the protein level of PER2 in mutant mice were found to increase earlier than in wild-type mice (**Figure 7**).

To test the effect of the *Per2* E'-box mutation on the other

clock genes, I investigated circadian mRNA expression profiles of *Per1*, *Per2*, *Per3*, *Cry1*, *Cry2*, *Clock*, *Npas2*, *Arntl1, Arntl2*, *Dbp*, *Nfil3*, *Rorα*, *Nr1d1*, *Bhlhe40* and *Bhlhe41* (**Figure 6e, 8**). Among the clock genes tested, *Per3* and *Npas2* showed an earlier circadian increase in their expression in mutant mice than in wild-type ones. These data suggest that altered PER2 affects circadian expression profiles of *Per3* and *Npas2*.

The current feedback model expects the repressor proteins PER and CRY to be recruited to the E-box elements in their target gene promoters[2]. I therefore hypothesized that the *Per2* E'-box might play an important role in recruitment of the circadian transcriptional repressors *in vivo*. To test this hypothesis, I performed chromatin immunoprecipitation (ChIP) assays. To detect chromatin binding of PER and CRY, I employed a dual crosslinking ChIP method[25, 35], which uses disuccinimidyl glutarate (DSG) prior to formaldehyde crosslinking. DSG has a longer spacer arm than formaldehyde and has been used to crosslink transcription factor (cofactor) protein-protein interactions on DNA[36]. Firstly, to validate the specificity of the method, ChIP assays for PER1, CRY1, and CRY2 were performed with the

mouse liver samples from wild-type (WT) and respective mutant mice (*Per1*$^{-/-}$, *Cry1*$^{-/-}$, and *Cry2*$^{-/-}$) (**Figure 9**). The results demonstrate that the antibodies I used for PER1, CRY1, and CRY2 immunoprecipitate the *Per2* E'-box fragment from WT sample more efficiently than the corresponding mutant. Then, to determine circadian binding profiles of the negative regulators to the *Per2* promoter E-box, WT mice were sacrificed every 4 hours over a 24-hr cycle in constant darkness (DD) and their liver samples were subjected to ChIP assays for PER1, CRY1, and CRY2 (**Figure 10**). The results revealed that PER1, CRY1, and CRY2 were all recruited to the *Per2* E'-box in a circadian time specific manner in the wild-type mouse liver. The recruitment of PER1 predominantly occurred at CT12 (**Figure 10a**). In comparison, CRY2 binding was observed from CT12 to CT20 (**Figure 10b**). On the other hand, CRY1 binding started to increase at CT20 with a peak at CT4 (**Figure. 10c**). Considering that *Per2* transcription reaches its maximum and minimum at CT16 and CT4, respectively (**Figure 2**), the negative regulators, PER1, CRY1, and CRY2, might play distinct roles in circadian transcriptional repression of *Per2* (see **Discussion**).

Finally, I tested whether the E'-box mutation abrogates the recruitment of PER1, CRY1, and CRY2 to the *Per2* promoter. I found that ChIP values of PER1, CRY1 and CRY2 were all reduced to near basal levels throughout the circadian cycle by the E'-box mutation (**Figure 10**), demonstrating that the E'-box is required for binding of the negative regulators. Based on these results, I conclude that the E'-box is responsible for circadian repression, rather than activation, of *Per2* transcription *in vivo*.

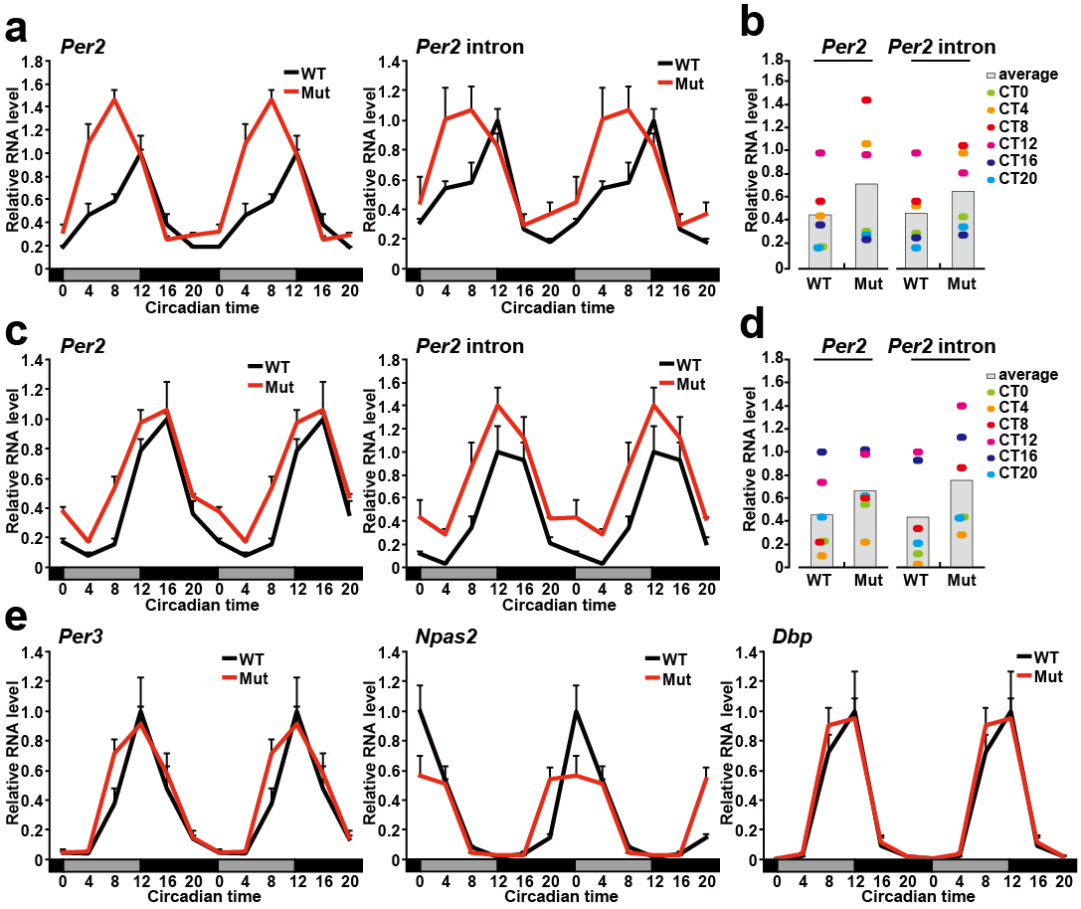

Figure 6. Increased abundance of *Per2* transcripts in mice bearing a mutation at the *Per2* promoter E'-box (−20/−15). a, *Per2* transcripts in the SCN of wild-type (WT) and *Per2* E'-box (−20/−15) mutant (Mut) mice. The levels of *Per2* mature (left) and immature (right) transcripts were determined by qRT-PCR. Data are shown in double plot, relative to wild-type peak values after normalization to *Rplp0*. Values are means ± s.e.m. (n = 3, for each data point). **b**, Comparisons of relative average values of 6 circadian time (CT) points of WT and Mut mice. The SCN *Per2* data shown in **a** are plotted. **c**, *Per2* transcripts in the liver of WT and Mut mice. Data were analyzed as described in **a**. **d**, Comparisons of relative average values of the liver *Per2* data shown in **c**. **e**, Circadian mRNA expression profiles of *Per3*, *Npas2*, and *Dbp* in the liver of WT and Mut mice. Data were analyzed as described in **a**. Also see **Figure 8**.

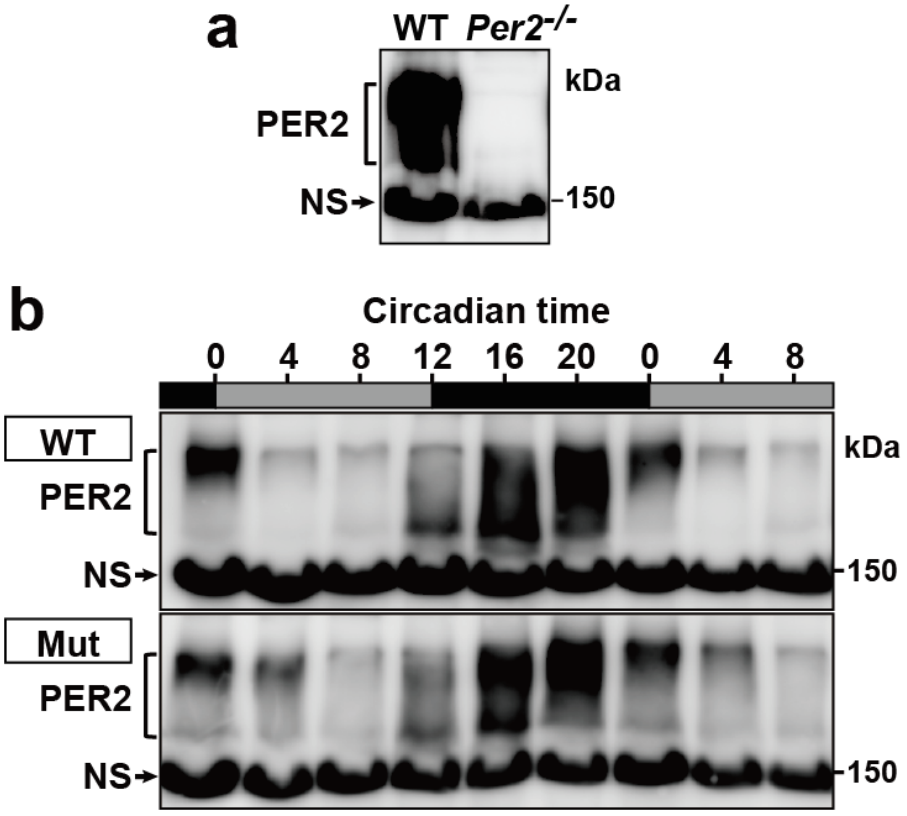

Figure 7. Altered protein expression of PER2 in mice carrying a mutation at the *Per2* E'-box (−20/−15). a, Immunoblotting of liver lysates from wildtype and *Per2*$^{-/-}$ mice with anti-PER2 antibody. NS, nonspecific band. **b**, Circadian profiles of PER2 protein abundance in liver lysates from wild-type (WT) and *Per2* E'-box (−20/−15) mutant (Mut) mice. Immunoblots of CT0, CT4, and CT8 were duplicated. NS, nonspecific band as loading control.

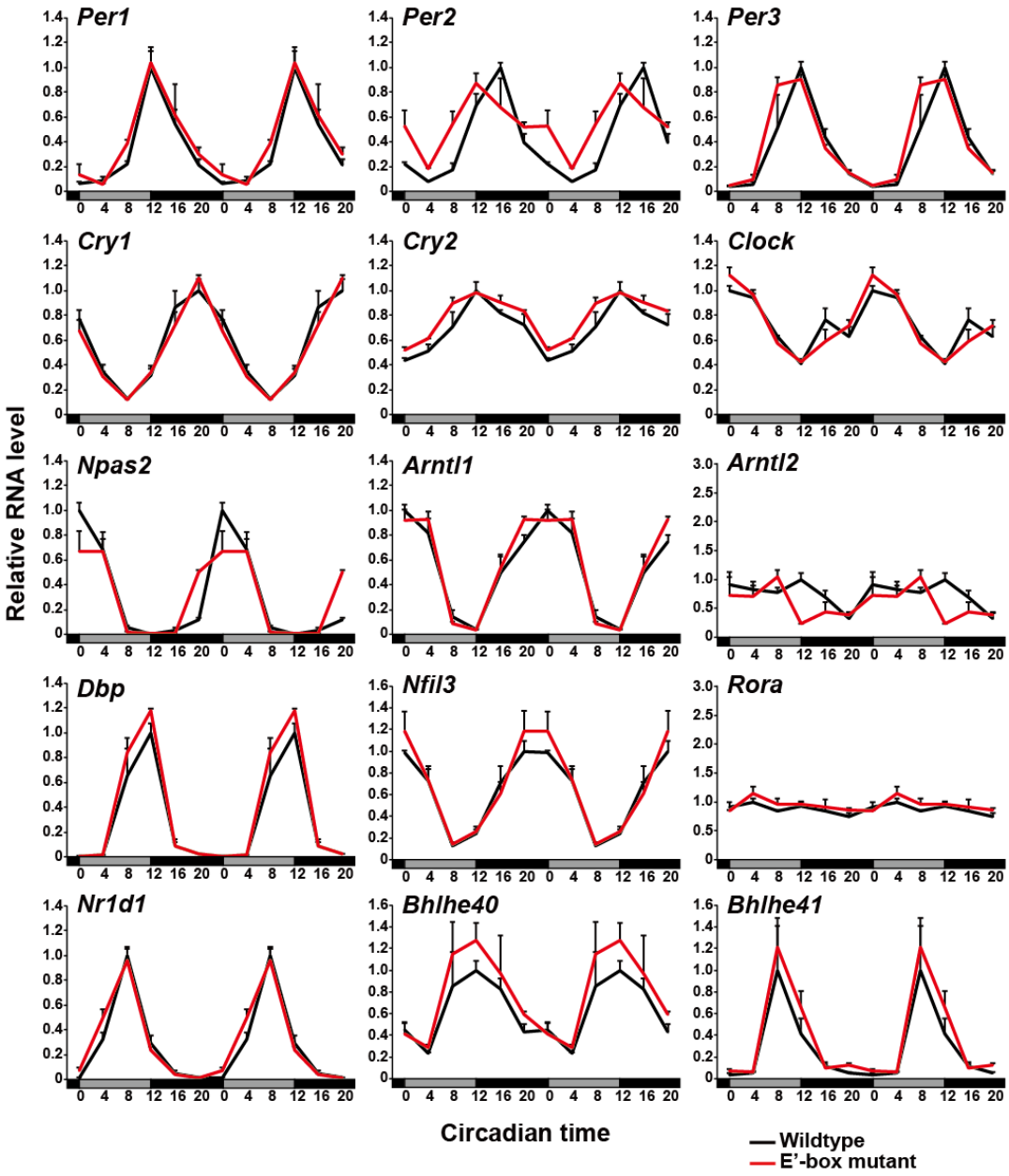

Figure 8. Expression of circadian clock genes in the livers from wildtype and *Per2* E'-box (−20/−15) mutant mice. Circadian expression profiles of 15 clock genes were determinded by qRT-PCR using a Fluidigm chip. Values are means ± s.e.m. (n = 3 mice for each data point) normalized to expression of ribosomal protein large P0 (Rplp0) gene. Data were double plotted.

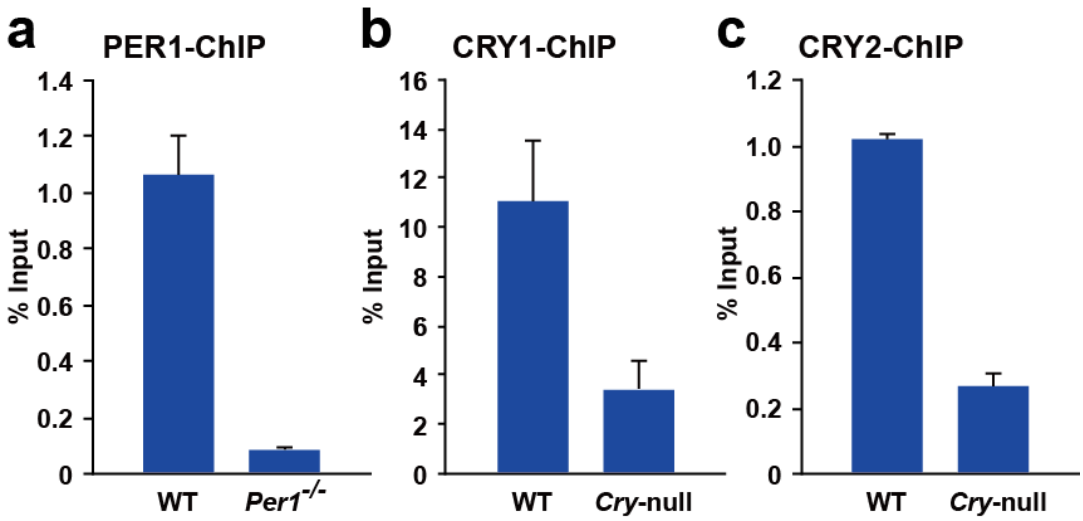

Figure 9. Specificity tests for the ChIP assays against PER1, CRY1, and CRY2. a, PER1-ChIP with liver samples from WT and *Per1*$^{-/-}$ mice at CT12. **b**, CRY1-ChIP with WT and *Cry*-null livers at CT0. **c**, CRY2-ChIP with WT and *Cry*-null at CT16. ChIP values (means ± s.e.m., n =3 for each data point) are shown relative to input DNA.

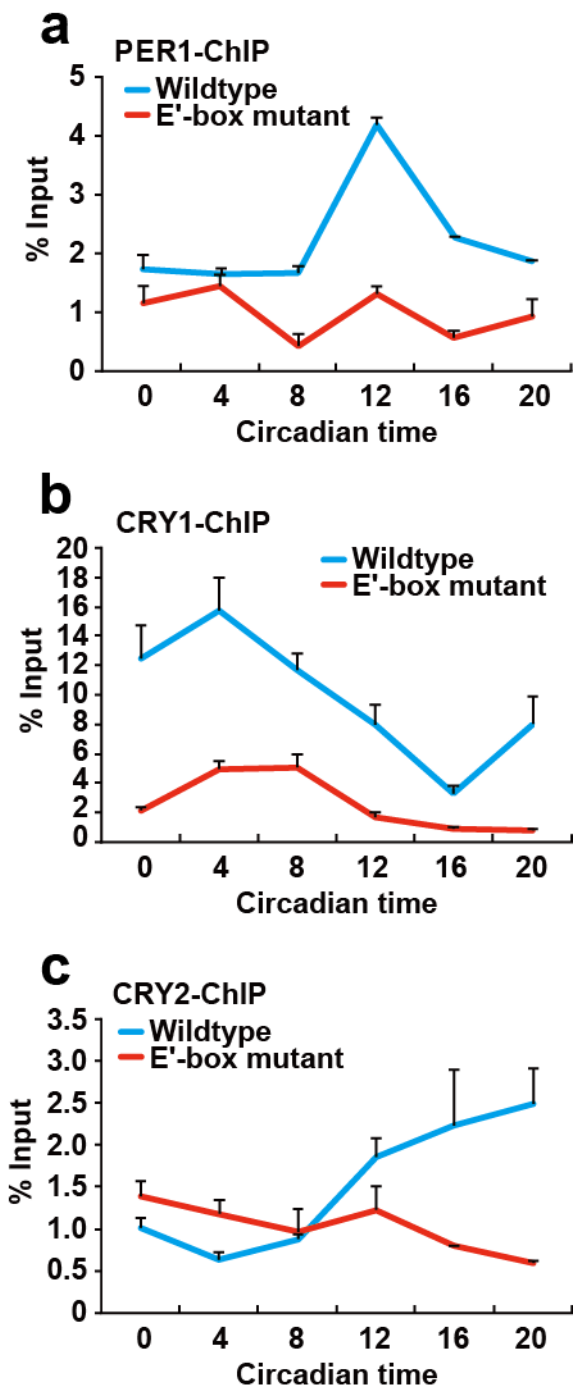

Figure 10. Impaired recruitment of the circadian repressor proteins to the *Per2* promoter in mice carrying a single mutation at the E'-box (−20/−15). ChIP assays for PER1 (**a**), CRY1 (**b**), and CRY2 (**c**) with liver samples from WT and *Per2* E'-box (−20/−15) mutant mice, sacrificed at 4-h intervals over a 24-h cycle in DD. ChIP values (means ± s.e.m., n = 2−3 for each data point) are shown relative to input DNA.

Discussion

The current feedback model expects the repressor proteins PER and CRY to be recruited to the E-box elements in their target gene promoters. However, a question remained unanswered as to when and how they are recruited to the target site *in vivo*. I performed dual crosslinking ChIP assay and determined circadian binding profiles of the repressor proteins, PER1, CRY1, and CRY2, to the *Per2* promoter E'-box. In a simple circadian model, these repressor proteins simultaneously bind to the E-box to repress transcription. However, this was not the case. The current study demonstrates that the *Per2* E'-box binding of PER1, CRY1, and CRY2 occurs in a sequential manner. There seems to be three separate circadian phases in repression, i.e., (i) an immediately early repressive phase (CT12-16) in which PER1 and CRY2 bind to the E-box to begin repression, (ii) an early repressive phase (CT16-24) in which CRY2 stays at the E-box to elicit repression, and (iii) a late repressive phase (CT0-8) in which CRY1 extends repression until the beginning of the next cycle of *Per2* expression. It is likely that these three sequential steps are required for determination of period for circadian repression.

I created mice carrying a point mutation of the *Per2* E'-box. The purpose of this study is to delineate the effect of this *in vivo* E'-box mutation on *Per2* circadian transcription. At present, available methods for gene targeting rely on positive selection to isolate rare clones that have undergone homologous recombination. To remove the unwanted selection cassettes, Cre/*loxP* or Flp/*FRT* recombination systems are used, which leave behind single *loxP* or *FRT* sites[31, 32]. These small ectopic sequences have the potential to interfere with transcriptional regulatory elements of surrounding genes[37]. To circumvent this problem, I employed the *piggyBac* transposon, a moth-derived DNA transposon, which can transpose efficiently in mammalian cells[29, 30]. A remarkable feature of this mobile element is seamless excision, which enables the removal of transgenes flanked by *piggyBac* inverted repeats without leaving any residual sequences[28, 30]. Taking advantage of this system, I have been able to create mice carrying a single E'-box mutation without introducing any unwanted sequences in the genome.

To evaluate whether the E'-box mutation *in vivo* abrogates rhythmicity of *Per2* expression, I determined circadian profiles of *Per2* mRNA in the mouse liver and SCN. Quantitative RT-PCR

analysis revealed that the point mutation of the *Per2* E'-box caused alteration of the circadian rhythm of *Per2*. This mutation impairs circadian repression of *Per2* expression and thereby elevates the levels of the baseline. Thus, the E'-box appears to be important for repression of *Per2* transcription *in vivo*. I therefore hypothesized that the *Per2* E'-box might play a role in recruitment of the negative circadian transcriptional regulators. To test this hypothesis, I performed dual crosslinking ChIP assays. In the wildtype mouse liver, the negative regulators, PER1, CRY1 and CRY2, were all recruited to the E'-box at the time of *Per2* repression. However, in the mutant mice, no recruitment was observed throughout the day, demonstrating that the *Per2* E'-box is required for binding of the negative regulators. Based on these results, I conclude that the E'-box is responsible for circadian repression, rather than activation, of *Per2* transcription *in vivo*.

Reference

1. Wijnen, H. & Young, M.W. Interplay of circadian clocks and metabolic rhythms. *Annual review of genetics* **40**, 409-448 (2006).
2. Takahashi, J.S., Hong, H.K., Ko, C.H. & McDearmon, E.L. The genetics of mammalian circadian order and disorder: implications for physiology and disease. *Nature reviews. Genetics* **9**, 764-775 (2008).
3. Dunlap, J.C. Molecular bases for circadian clocks. *Cell* **96**, 271-290 (1999).
4. Schibler, U. & Sassone-Corsi, P. A web of circadian pacemakers. *Cell* **111**, 919-922 (2002).
5. Reppert, S.M. & Weaver, D.R. Coordination of circadian timing in mammals. *Nature* **418**, 935-941 (2002).
6. Liu, A.C., Lewis, W.G. & Kay, S.A. Mammalian circadian signaling networks and therapeutic targets. *Nature chemical biology* **3**, 630-639 (2007).
7. Hastings, M.H., Maywood, E.S. & O'Neill, J.S. Cellular circadian pacemaking and the role of cytosolic rhythms. *Curr Biol* **18**, R805-R815 (2008).
8. Okamura, H., Yamaguchi, S. & Yagita, K. Molecular machinery of the circadian clock in mammals. *Cell Tissue Res* **309**, 47-56 (2002).
9. Tomoda, A. et al. Case study: differences in human Per2 gene expression, body temperature, cortisol, and melatonin parameters in remission and hypersomnia in a patient with recurrent hypersomnia. *Chronobiology international* **20**, 893-900 (2003).
10. Zheng, B. et al. The mPer2 gene encodes a functional component of the mammalian circadian clock. *Nature* **400**, 169-173 (1999).

11. Toh, K.L. et al. An hPer2 phosphorylation site mutation in familial advanced sleep phase syndrome. *Science* **291**, 1040-1043 (2001).
12. Fu, L., Pelicano, H., Liu, J., Huang, P. & Lee, C. The circadian gene Period2 plays an important role in tumor suppression and DNA damage response in vivo. *Cell* **111**, 41-50 (2002).
13. Albrecht, U., Sun, Z.S., Eichele, G. & Lee, C.C. A differential response of two putative mammalian circadian regulators, mper1 and mper2, to light. *Cell* **91**, 1055-1064 (1997).
14. Takumi, T. et al. A light-independent oscillatory gene mPer3 in mouse SCN and OVLT. *EMBO J* **17**, 4753-4759 (1998).
15. Yamaguchi, S. et al. The 5' upstream region of mPer1 gene contains two promoters and is responsible for circadian oscillation. *Curr Biol* **10**, 873-876 (2000).
16. Yamamoto, T. et al. Acute physical stress elevates mouse period1 mRNA expression in mouse peripheral tissues via a glucocorticoid-responsive element. *The Journal of biological chemistry* **280**, 42036-42043 (2005).
17. Doi, M., Okano, T., Yujnovsky, I., Sassone-Corsi, P. & Fukada, Y. Negative control of circadian clock regulator E4BP4 by casein kinase Iepsilon-mediated phosphorylation. *Curr Biol* **14**, 975-980 (2004).
18. Yamamura, K. et al. Immunolocalization of murine type VI 3beta-hydroxysteroid dehydrogenase in the adrenal gland, testis, skin, and placenta. *Mol Cell Endocrinol* **382**, 131-138 (2014).
19. Nakanishi, H., Higuchi, Y., Kawakami, S., Yamashita, F. & Hashida, M. piggyBac transposon-mediated long-term gene expression in mice. *Mol Ther* **18**, 707-714 (2010).

20. Yagi, T. et al. A novel ES cell line, TT2, with high germline-differentiating potency. *Analytical biochemistry* **214**, 70-76 (1993).
21. Rad, R. et al. PiggyBac transposon mutagenesis: a tool for cancer gene discovery in mice. *Science* **330**, 1104-1107 (2010).
22. Markel, P. et al. Theoretical and empirical issues for marker-assisted breeding of congenic mouse strains. *Nature genetics* **17**, 280-284 (1997).
23. Wakeland, E., Morel, L., Achey, K., Yui, M. & Longmate, J. Speed congenics: a classic technique in the fast lane (relatively speaking). *Immunology today* **18**, 472-477 (1997).
24. Suemizu, H. et al. Establishing EGFP congenic mice in a NOD/Shi-scid IL2Rg(null) (NOG) genetic background using a marker-assisted selection protocol (MASP). *Experimental animals / Japanese Association for Laboratory Animal Science* **57**, 471-477 (2008).
25. Ota, T. et al. Angiotensin II triggers expression of the adrenal gland zona glomerulosa-specific 3β-hydroxysteroid dehydrogenase isoenzyme through de novo protein synthesis of the orphan nuclear receptors NGFIB and NURR1. *Mol Cell Biol* **34**, 3880-3894 (2014).
26. Yoo, S.H. et al. A noncanonical E-box enhancer drives mouse Period2 circadian oscillations in vivo. *Proc Natl Acad Sci U S A* **102**, 2608-2613 (2005).
27. Akashi, M., Ichise, T., Mamine, T. & Takumi, T. Molecular mechanism of cell-autonomous circadian gene expression of Period2, a crucial regulator of the mammalian circadian clock. *Mol Biol Cell* **17**, 555-565 (2006).

28. Fraser, M.J., Ciszczon, T., Elick, T. & Bauser, C. Precise excision of TTAA-specific lepidopteran transposons piggyBac (IFP2) and tagalong (TFP3) from the baculovirus genome in cell lines from two species of Lepidoptera. *Insect Mol Biol* **5**, 141-151 (1996).
29. Ding, S. et al. Efficient transposition of the piggyBac (PB) transposon in mammalian cells and mice. *Cell* **122**, 473-483 (2005).
30. Wang, W. et al. Chromosomal transposition of PiggyBac in mouse embryonic stem cells. *Proc Natl Acad Sci U S A* **105**, 9290-9295 (2008).
31. van der Weyden, L., Adams, D.J. & Bradley, A. Tools for targeted manipulation of the mouse genome. *Physiol Genomics* **11**, 133-164 (2002).
32. Hockemeyer, D. et al. Efficient targeting of expressed and silent genes in human ESCs and iPSCs using zinc-finger nucleases. *Nat Biotechnol* **27**, 851-857 (2009).
33. Yusa, K., Rad, R., Takeda, J. & Bradley, A. Generation of transgene-free induced pluripotent mouse stem cells by the piggyBac transposon. *Nat Methods* **6**, 363-369 (2009).
34. Yusa, K. et al. Targeted gene correction of α1-antitrypsin deficiency in induced pluripotent stem cells. *Nature* **478**, 391-394 (2011).
35. Zeng, P.Y., Vakoc, C.R., Chen, Z.C., Blobel, G.A. & Berger, S.L. In vivo dual cross-linking for identification of indirect DNA-associated proteins by chromatin immunoprecipitation. *BioTechniques* **41**, 694, 696, 698 (2006).
36. Tian, B., Yang, J. & Brasier, A.R. Two-step cross-linking for analysis of protein-chromatin interactions. *Methods Mol Biol* **809**, 105-120 (2012).

37. Meier, I.D. et al. Short DNA sequences inserted for gene targeting can accidentally interfere with off-target gene expression. *FASEB journal : official publication of the Federation of American Societies for Experimental Biology* **24**, 1714-1724 (2010).

Acknowledgements

First of all, I wish to express sincere thanks to Prof. H. Okamura and Dr. M. Doi for their direction and kind encouragement throughout my graduate study.

I thank Prof. M. Hashida (Kyoto University, Kyoto), who kindly provided the DNA construct encoding a *piggyBac* terminal repeat, Prof. A. Bradley (Wellcome Trust Sanger Institute, UK) for providing the ROSA26-PBase mice, Dr. C. Lee (Florida State University, USA) for providing anti-CRY1 and anti-CRY2 antibodies, and Dr. N. Koike (Kyoto Prefectural University of Medicine, Kyoto) for technical advice in the ChIP assay.

I am grateful to all the member of Okamura's lab for their advice and help. In particular, I appreciate the technical assistance and contributions of Mr. H. Hayashi.

I thank my parents for their support and encouragement. Without their support I would not have accomplished this thesis.